Superconducting Parameters and Size Effects of Aluminum Films and Foils*

M. David Maloney,† Francisco de la Cruz,‡ and Manuel Cardona§
Department of Physics, Brown University, Providence, Rhode Island 02912
(Received 23 August 1971)

In this paper we present the experimental results and analysis of the critical-field determination of aluminum films and foils. We studied the thermodynamic parallel and perpendicular critical fields as a function of thickness and temperature. The measurement of the critical fields together with suitable theories allows the determination of the penetration depth λ, the coherence length ξ, and the surface-energy parameter Δ. The thermodynamic transition of all films studied was of second order. Measurement in both magnetic field orientations offers a check on the consistency of the methods used to analyze the data. The value of the Ginzburg-Landau parameter κ obtained from these measurements is six times larger than the value obtained from supercooling experiments. This phenomenon has been observed previously by other authors in different metals. The superconducting transition of all foil samples was of first order. In perpendicular fields the transition to the intermediate state was analyzed by means of an interpolation formula having the correct theoretical behavior in the limits of both large and small thicknesses. The value of the surface-energy parameter so obtained is in agreement with the supercooling result.

I. INTRODUCTION

The measurement of the parallel $H_{\parallel}$ and perpendicular $H_{\perp}$ critical fields of thin superconducting films can be used to determine the penetration depth λ and coherence length ξ of a type-I superconductor. These quantities determine the Ginzburg-Landau (GL) parameter κ of the material. Another method to obtain κ is to measure the supercooling of "ideal" bulk samples and to use the Ginzburg relation[1] between the supercooling and critical fields.

An extensive investigation of the normal-superconducting transitions in magnetic fields of both orientations ($\parallel$ and $\perp$) for Pb and Sn films and foils has been made by Cody and Miller.[2,3] Other measurements for the perpendicular orientation in thin and thick films have also been made for Sn,[4,5] In,[4,6] and most recently for Al.[6] Measurements of the ideal supercooling fields of those materials are also available.[7–9] A comparison of the results for κ using both methods is shown in Table I. A discrepancy, first found by Cody and Miller,[2,3] can be seen for all materials listed. It appears clearly in Table I that the values of κ obtained from supercooling measurements are systematically smaller than those obtained from film experiments. It is noteworthy that the difference between the two determinations increases when κ decreases. Initially the Cody-Miller results[2,3] prompted our work with Al in order to understand this difference. During the course of this experiment, results for the perpendicular critical field of Al films were published.[6] In this paper we include our results for this geometry as a matter of completeness and because our analysis is somewhat different.

The theoretical treatment of thin films in parallel magnetic fields is available,[10,11] but no theory has been developed for the perpendicular direction in the nonlocal case. Under the assumption that mean free path (mfp) and size effects are equivalent,[12] several semiempirical expressions[2,3,12] for $H_{\perp}$ as a function of thickness have been used. Hence measurements of $H_{\parallel}$ in addition to $H_{\perp}$ are very useful for checking the consistency of a particular method of analysis.

For thick-enough samples of type-I materials the transition in a perpendicular field is to the intermediate state. We denote as $H_{\perp}^{D}$ the critical field at which these samples become completely normal. The study of the variation of $H_{\perp}^{D}$ with thickness allows one to determine the surface-energy parameter.[2,3,6,12] It is also possible to find the critical thickness at which the transition changes from first to second order. A theoretical study by Lasher[13] of the stability of the solution to the GL equation for a second-order transition predicts a decrease of the critical thickness D_c towards zero as κ goes to zero. The data analysis by Cody and

TABLE I. Supercooling and thin-film results for κ.

	κ_{sc}	$\kappa_{\perp}$
Pb	0.24[a]	0.37[b]
Sn	0.087[a]	0.15[c]
	0.093[d]	0.22[e]
In	0.06[a,d]	0.11[c]
		0.19[f]
Al	0.015[g]	0.085[h]

[a]Reference 8.
[b]Reference 2.
[c]Reference 4.
[d]Reference 7.
[e]Reference 3.
[f]Reference 6.
[g]Reference 9.
[h]This work.

Miller,[2,3] and more recently by Brandt *et al.*,[6] does not support the Lasher theory.[13]

The value of κ depends on the purity of the material. Consequently, it is necessary to determine the electron mfp for the samples under investigation. We measured the electrical resistivity of our samples and found that corrections for impurity effects would be necessary in the case of our film samples. Using the theory for $H_{\parallel}$ and a semiempirical relation for $H_{\perp}$ we are able to separate size effects from impurity effects. With appropriate corrections for both, a determination of the κ for pure Al is possible. The values obtained from each set of independent data, i.e., from $H_{\perp}$ and $H_{\parallel}$, are coincident, within the experimental error. We get $\kappa = 0.086$, nearly six times larger than the value obtained from the supercooling experiment.[9]

Our measurements of $H_{\perp}^{D}$ as a function of thickness for pure aluminum foils show that the theoretical expression commonly used[2,3,6] to fit experimental data is not adequate over most of the range of sample thicknesses. However, in the limit of large thickness where it should be valid, the expression does give the correct description when the supercooling value for κ is used.

II. THEORETICAL APPROACH

Here we present the theoretical and semiempirical expressions used to analyze the results. We emphasize that bulk mfp effects were important in our film samples. Where confusion might arise we explicitly include in our notation the mfp (l) and thickness (d) dependence of the superconducting parameters [i.e., $\kappa(l,d)$, $\lambda(l,d)$, $\xi(l,d)$].

A. Films: Parallel Orientation

The solution of the GL equation for a semi-infinite sample with the field parallel to the surface is given by[1,14]

$$H_{\parallel} = 2.4\,\kappa H_c\,, \tag{1}$$

where H_c is the critical field of the bulk material. In a type-I superconductor H_c is larger than $H_{\parallel}$ and the solution corresponds to a metastable thermodynamic state. If the same is a plate of thickness approaching the order of the penetration depth, the relative contribution of the positive magnetic energy to the total free energy decreases and the critical magnetic field $H_{\parallel}$ increases. Eventually, for a thickness smaller than a critical one, the stable solution of the appropriate GL equation will correspond to a field larger than H_c. When this thickness is achieved the normal-superconducting transition is a thermodynamic second-order transition. Studying the stability of the solution as a function of thickness, Ginzburg and Landau[15] found that below a critical thickness the solution of the GL equation in the limit $d \ll \xi(t,l,\infty)$ is

$$H_{\parallel} = \sqrt{24}\, H_c \lambda(t,l,\infty)/d\,, \tag{2}$$

where t is the reduced temperature. Expression (2) has received strong qualitative experimental support but no quantitative agreement has been found. (See Refs. 10 and 16 for a review of the theoretical and experimental work.) The reason for the quantitative failure of Eq. (2) is that the GL equations imply the locality of the electrodynamics, that is, the penetration depth must be large compared with the Pippard coherence length, defined by $\xi_p^{-1} = \xi_0^{-1} + l^{-1}$. For bulk samples this condition is always achieved at temperatures sufficiently close to T_c. For a thin film the length over which the field varies is set by the size of the sample. If ξ_p is larger than this, nonlocal effects will appear at all temperatures.[10] The effect of the nonlocal electrodynamics is to make the penetration depth in Eq. (2) thickness dependent. Nonlocal corrections to Eq. (2) have been found in several limits.[11] Since the mfp of our films is $l \leq d$, none of the limiting expressions are useful. Thompson and Baratoff[10] have developed a theory valid for any relation of mean free path to sample dimensions. We assume diffuse boundary scattering and use the corresponding theoretical expressions.

Using the results of Ref. 10 it is possible to write

$$\frac{H_{\parallel}(t,l,d)}{H_c(t,l,\infty)} = \frac{\pi^2 \lambda_{\mathrm{eff}}(l,d)}{2d}\, F(t)\,, \tag{3}$$

where $F(t)$ contains the temperature dependence of λ_{eff} with $F(0) = 1$ and λ_{eff} is an effective penetration depth given by

$$\lambda_{\mathrm{eff}}(l,d) = \frac{f^{-1/2}(\xi_p(l,\infty)/d)}{\chi^{1/2}(\xi_0/l)}\, \lambda_L\,. \tag{4}$$

λ_L is the London penetration depth, χ is the Gor'kov correction[17] for mfp effects, and $f(\xi_p/d)$ is a correction for nonlocality computed by Thompson and Baratoff for diffuse scattering.[10]

Equation (4) involves both the coherence length and the penetration depth. In order to use the experimental $H_{\parallel}$ to determine one of the parameters, it is convenient to transform Eq. (4) using $H_c(t,\infty,\infty) = \phi_0/[2\pi\sqrt{2}\lambda(t)\,\xi(t)]$ into

$$H_{\parallel}(t,l,d) = \frac{1.05\times10^{-7} f^{-1/2}(\xi_p/d)}{d\,\chi^{1/2}}\, \frac{T_c}{T_{cB}}\, \frac{1}{\xi_0}\, F'(t), \tag{5}$$

where $F'(t)$ contains the temperature dependence, $F'(0) = 1$, and T_{cB} is the critical temperature of an infinite pure sample. In Eq. (5) we have introduced the factor T_c/T_{cB} to take into account possible differences between the critical temperature of the film and that of the bulk; it assumes that a change in the critical temperature requires a critical-field adjustment $H_c(t,l) = H_c(t,\infty)\, T_c/T_{cB}$. By fitting the experimental thickness or temperature dependence

of $H_{\parallel}$ with Eq. (5), one can determine the pure temperature-independent coherence length ξ_0. Replacing the obtained value of ξ_0 in Eq. (4) one can determine $\lambda_L(0)$ and consequently the GL parameter κ of the pure bulk metal.

B. Films: Perpendicular Orientation

Tinkham[18] has shown that the perpendicular critical field for films can be expressed by

$$H_{\perp}(t, l, d) = \sqrt{2}\kappa_{\perp}(t, l, d)\, H_c(t, l), \tag{6}$$

provided the film is thin enough to have a second-order superconductive transition. The thickness dependence of the critical field is introduced through an effective GL parameter $\kappa_{\perp}$. This parameter can be determined experimentally if $H_{\perp}$ and H_c are measured. We are also interested in obtaining from these data the GL parameter of the bulk material, in order to compare it with the results from the parallel orientation. As in the parallel case a nonlocal theory separating the size from the mfp effects is required in order to analyze the data. No such theory is available, but several semiempirical expressions have been proposed.[2,3,6,12]

It is generally assumed that the effect of the boundaries can be taken into account by using an effective size-dependent electron mfp in the Gor'kov function χ.[17] For the effective mfp one uses the Fuchs's relation

$$\rho(l, d) = \rho(l, \infty)\, \zeta(l/d), \tag{7}$$

where $\zeta(l/d)$ has been computed and plotted by Fuchs.[19] The impurity mfp l is determined by fitting the measurements of the electrical resistivity as a function of thickness at He temperatures to the appropriate Fuchs relation.

From the effective χ a functional dependence of $\kappa_{\perp}$ on d can be found. If the experimental data fit the proposed d dependence, an extrapolation to $d \to \infty$ should give the bulk GL parameter desired for a comparison with the value from the parallel geometry. Let us mention here that when a sample is thick enough the transition is to an intermediate state, and Eq. (6) for $H_{\perp}$ should describe the supercooling field for the perpendicular orientation.

C. Foils: Perpendicular Orientation

We have discussed the method of analysis when the transition is of second order. For thick-enough samples the superconducting transition at the perpendicular field $H_{\perp}^{D}$ is to the intermediate state. Taking into account the contribution of the positive surface energy it is possible to show[20] that $H_{\perp}^{D}$ decreases as the thickness diminishes. In the approximation that the thickness is much larger than the temperature-dependent coherence length $\xi(t)$, one finds[20]

$$H_{\perp}^{D} = H_c\left[1 - \frac{4\phi^{1/2}}{1-\eta}\left(\frac{\Delta}{d}\right)^{1/2}\right]^{1/2}. \tag{8}$$

In Eq. (8) Δ is the surface-energy parameter and ϕ is a function of $\eta = H_0/H_c$, where H_0 is the applied field. The function ϕ takes into account the contribution to the free energy due to the distortion of the superconducting domains at the surface of the sample. Lifshitz and Sharvin[21] have computed this function for the Landau model[22] of the intermediate state. Within this model and for $\eta \to 1$, Eq. (8) can be written[20]

$$H_{\perp}^{D} = H_c\left[1 - 1.88\left(\frac{\Delta}{d}\right)^{1/2}\right]^{1/2}, \tag{9}$$

which is usually expanded when $d \gg \Delta$ to the familiar form

$$H_{\perp}^{D} \simeq H_c\left[1 - \left(\frac{C\Delta}{d}\right)^{1/2}\right], \tag{10}$$

where $C = 0.88$. Similar expressions have been found[12,23] for other models of the intermediate state. Cody and Miller[2,3] have used Eq. (10) and Brandt *et al.*[6] have used Eq. (9) together with the experimental values of $H_{\perp}^{D}$ to obtain the surface parameter Δ for different metals. Once Δ is determined, one uses a measured value of λ to evaluate κ from relations given by Ginzburg[24] or Bardeen.[25] Thus a study of the intermediate state of foils in a transverse field offers another method of obtaining a κ to be compared with thin-film and supercooling results.

III. EXPERIMENTAL METHOD

Foils were rolled from sheets of 99.999%-pure Al supplied by A. D. MacKay, Inc. Specimens were placed between 0.002-in. Mylar to prevent contact with the stainless-steel rollers, and then cut with a razor blade to the appropriate dimensions of 2.5×8 mm. The thicknesses of eight samples between 172 and 3 μ were determined by weighing. Four of these were also checked by measuring the room-temperature and helium-temperature resistances.

Thin films were vacuum deposited on room-temperature glass substrates of the same 2.5×8-mm geometry from bulk pieces of 99.995%-pure Al from Johnson Matthey, Ltd. We maintained the pressure below 5×10^{-6} Torr while evaporating at a rate of about 20 Å/sec. Seven films were prepared, ranging in thickness from 1.1 μ to 1425 Å. The thicknesses were determined from resistance measurements. Past attempts to measure the thickness with an interferometer have led to inconsistencies[26] and to the preference of the resistance method.

Both films and foils were annealed for 4 days at 400 °C under a pressure of less than 10^{-7} Torr. The transition widths in zero magnetic field were 1–3 mK for all foils. For the films the transition

width showed some inverse thickness dependence, ranging from 15 mK for the thickest to 45 mK for the thinnest. Further annealing produced no change in the transition width.

The resistivity ρ of each sample was measured by means of a standard four-probe dc technique. From the results at room temperature and at 4.2 °K the sample thickness was determined with the expression

$$d = \frac{\rho_{293}}{R_{293} - R_{4.2}} \frac{L}{W}, \tag{11}$$

where $\rho_{293} = 2.7 \times 10^{-6}$ Ω cm is the intrinsic resistivity of pure bulk Al at room temperature, R_{293} and $R_{4.2}$ are the resistances measured at two temperatures, and L and W are the length and width of the sample.

Using Fuchs's relation[19] between resistivity and sample thickness, we obtained values for the bulk mfp l and for the constant ρl. For the rolled samples $l = 171 \pm 15$ μ and $\rho l = (10.8 \pm 1.3) \times 10^{-12}$ Ω cm^2. The evaporated samples have $l = 0.15 \pm 0.05$ μ and $\rho l = (18 \pm 7) \times 10^{-12}$ Ω cm^2. This is to be compared with literature values of $\rho l = 7 \times 10^{-12}$ Ω cm^2 by Cotti *et al.*[27] and $\rho l = 8 \times 10^{-12}$ Ω cm^2 measured by Holwech and Jeppesen[28] for very-high-purity Al. In fact it has been suggested that ρl is a function[28–30] of the resistivity ratio. For a ratio of 4000, which we have for an infinitely thick foil, the literature value[29] is indeed $\rho l \sim 11 \times 10^{-12}$ Ω cm^2. Bassewitz and Mitchell[30] have pointed out that evaporated films of Al due to their much lower ratios have a higher value of ρl than that of pure Al. This fact is consistent with our results in spite of their large experimental error. We should also note that both Al supplies (A. D. McKay and Johnson Matthey) gave the same value of ρl in the bulk.

The superconductivity of our samples was detected by an ac susceptibility method. The sample was placed between the primary and secondary coils of a mutual inductance bridge, so that the presence of supercurrents would shield the secondary coil from the ac probing field. The plane of the sample was normal to this ac field, thereby optimizing the shielding effects. The primary field was less than 0.1 Oe and the frequency used was 1000 Hz.

We monitored both the real and imaginary parts of the susceptibility as a function of the external dc magnetic field, which could be oriented either parallel or perpendicular to the plane of the sample. The real part χ', which designates the change in the mutual inductance of the coils, was used to determine the critical fields of the samples. The imaginary part χ'', proportional to the ac losses in the sample, showed a sharp maximum coincident with the critical field whenever the transition was sharp. However, thick samples in the perpendicular orientation go into the intermediate state at very low fields, and the transition is broad. Cody and Miller[2,3] have pointed out that the peak in the imaginary part of the susceptibility is inadequate to define the critical field in this case. We indicate in Fig. 1 our definitions of the parallel and perpendicular critical fields. These definitions mark the limiting traces of shielding by the supercurrents.

We were able to locate the parallel orientation within 0.1°, and also to ensure the absence of errors due to the earth's magnetic field.

The critical temperature was determined by plotting the critical field as a function of temperature, and extrapolating the data to $H = 0$. The onset of superconductivity in the zero magnetic field was generally sharp and always coincided with the above extrapolation within experimental error. For the foils the transition temperature decreased slightly with decreasing thickness, giving qualitative agreement with the anisotropy-averaging model of Markowitz and Kadanoff.[31] The data extrapolate for infinite thickness to a value of $T_c = (1.181 \pm 0.001)$ °K $\equiv T_{cB}$. The thin-film results for T_c as a function of thickness are shown in Fig. 2. The critical temperature now increases with decreasing thickness, an effect possibly related to that reported by Khukhareva[32] and Strongin *et al.*[33] under similar sample conditions.

Trimming the edges of our film samples had no effect on the transition temperatures or the critical fields as a function of temperature. The tails of the transitions in zero and nonzero fields were more extended before the edges were cut.

To obtain the temperatures required for this experiment (1.4–0.5 °K), we used a He^3 cryostat designed so that the sample and test coils were immersed in the liquid. The thermometer was a 12-Ω, $\frac{1}{10}$-W Allen-Bradley carbon resistor, calibrated against the He^3 vapor pressure. The temperature was monitored by an ac resistance bridge, and could be stabilized within ± 0.5 mK.

IV. RESULTS

The parallel and perpendicular critical fields were measured as a function of temperature (from T_c to 0.5 °K) and thickness (from 172 μ to 1425 Å). The size effects were such that the films undergo a second-order transition, while the foil transitions are clearly first order. Indeed, the film transitions have no hysteresis and the foils show large supercooling. The amount of supercooling varies from sample to sample and is always less than the ideal one found for spheres.[9]

A. Parallel Orientation

1. *Foils*

In Fig. 3 we plot the parallel critical field as a function of temperature for the 23-μ sample. The dashed line through the experimental points repre-

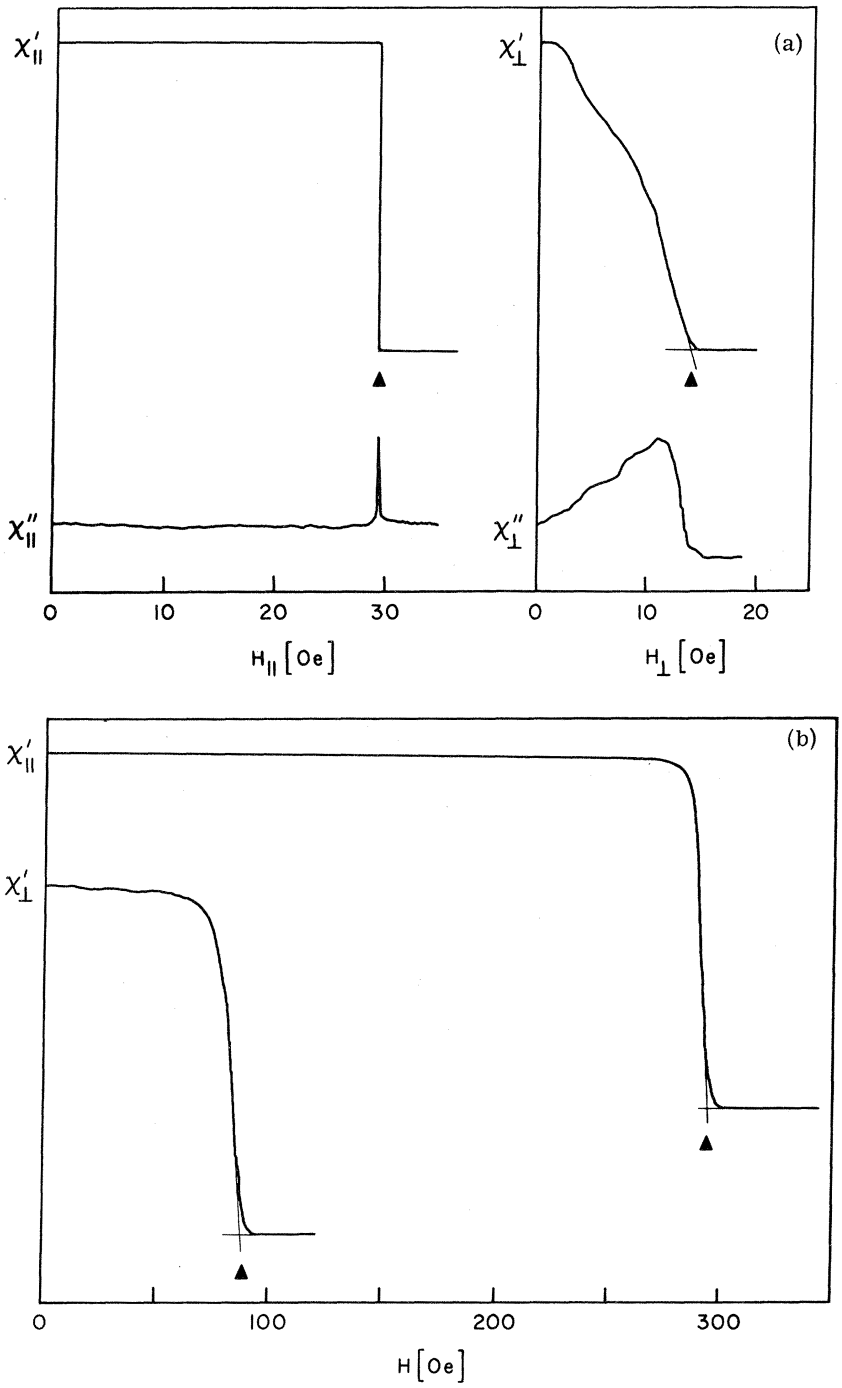

FIG. 1. Mutual-inductance curves for (a) 6.4-μ foil at a reduced temperature of $t=0.828$, (b) 1750-Å film at $t=0.374$. The ordinate represents the real part χ' and the imaginary part χ'' of the susceptibility in arbitrary units for magnetic field orientations both parallel and perpendicular to the sample plane. Triangles indicate the critical fields chosen.

sents the measurements of $H_c(T)$ by Harris and Mapother[34] on bulk Al. We adjust their curve according to the law $H_c(0)/T_c = \text{const}$. The agreement between the dashed line in Fig. 3 and our points indicates that this scaling factor is correct, within our accuracy. Figure 3 also shows no indication of size effects for this sample. We find this fact to hold for all but the thinnest foil: The critical field of the 3.1-μ specimen exceeds H_c by about 3% near T_c, indicating the beginning of a size effect.

2. *Films*

Figure 4 is a plot of $H_{\parallel}$ as a function of either $[(1-t^2)/(1+t^2)]^{1/2}$ or $(1-t^2)/(1+t^2)$ for three films. The particular function of temperature involved in each case depends on the sample thickness d as

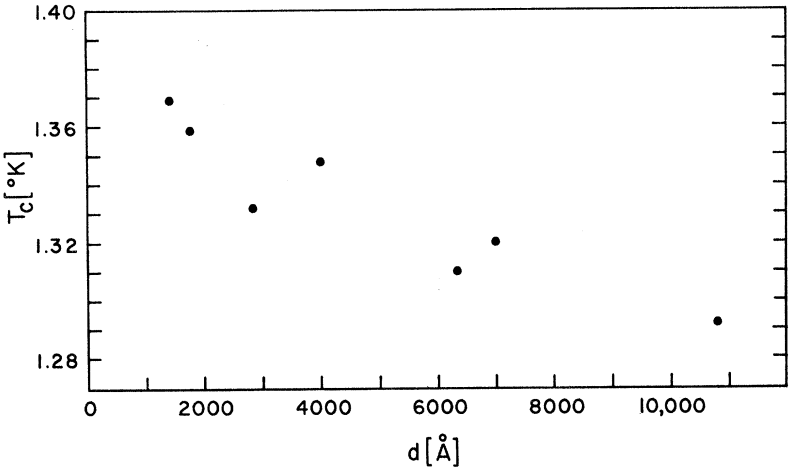

FIG. 2. Critical temperature of Al films as a function of thickness d.

compared to the penetration depth $\lambda_{eff}(t)$ and to the coherence length $\xi(l,t)$. This phenomenon, as well as the specific dependence of $H_{\parallel}$ on d, is discussed in Sec. V. The most noticeable general feature is the rapid increase in $H_{\parallel}$ as the thickness decreases. For the thinner samples we note that $H_{\parallel}^2$ is linear in t near $t=1$. For all films the ratio $H_{\parallel}/H_c$ was found to be proportional to $(1-t^4)^{-1/2}$ near $t=1$ [that is, in Eq. (3) we have $F(t)=(1-t^4)^{-1/2}$ within experimental error]. The slopes α of $H_{\parallel}/H_c$ vs $(1-t^4)^{-1/2}$ are listed in Table II. Here again we have computed H_c from the data of Harris and Mapother[34] by adjusting for the T_c of each film.

The linear portion of $H_{\parallel}$ vs $[(1-t^2)/(1+t^2)]^{1/2}$ [see Figs. 4(a) and 4(b)] occurs when $H_{\parallel}/H_c > 2.2$. Greater thicknesses and lower temperatures have the effect of lowering $H_{\parallel}/H_c$. For $H_{\parallel}/H_c < 2.2$, the points leave the straight line. In Table II we listed the slopes β of the linear portion for each film. In this case ($H_{\parallel}/H_c > 2.2$) we use Eq. (5) to evaluate the BCS coherence length ξ_0 from these slopes. The thickest film (1.08 μ) is omitted since $H_{\parallel}/H_c < 2.2$ even for temperatures as high as $t=0.95$, and Eqs. (3) and (5) are no longer valid. Note that within experimental error we have the two-fluid-model temperature dependence usually observed[11] {that is, in Eq. (5) $F'(t)=[(1-t^2)/(1+t^2)]^{1/2}$}. The average for six of the films is $\xi_0 = 0.49 \pm 0.07$ μ. This value of ξ_0 is considerably smaller than that obtained from supercooling in spheres[9] ($\xi_0 = 1.2$ μ) and the free-electron BCS value ($\xi_0 = 0.18\hbar v_F = 1.6$ μ). The discrepancy between the BCS value and that from supercooling in spheres has been attributed to Fermi-surface anisotropy. To evaluate ξ_0 from the slope β we have used the measured thickness d and the transition temperature T_c for each film. Since f and χ are functions of the Pippard and BCS coherence lengths, respectively, Eq. (5) was solved graphically for ξ_0. From this known value of ξ_0, we make use of the slopes α in Table II and Eqs. (3) and (4) to determine the London penetration depth $\lambda_L(0)$ for each film. The result for six films is $\lambda_L(0) = 440 \pm 30$ Å. For the thick films at low temperatures $H_{\parallel}$ vs $(1-t^2)/(1+t^2)$ becomes linear through the origin [see Figs. 4(c) and 4(d)]. This is the two-fluid-model temperature dependence of bulk type-II superconductivity, that is,[35]

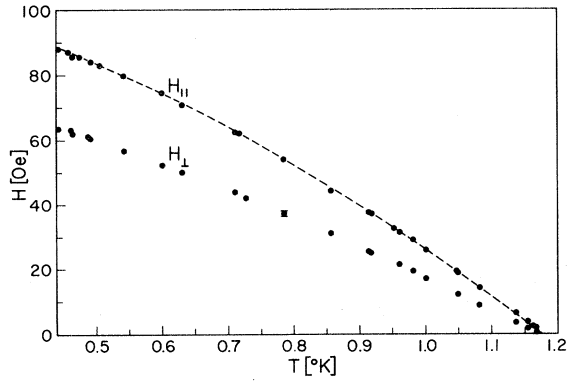

FIG. 3. Parallel and perpendicular critical fields of a 23-μ foil as a function of temperature T. Dashed curve represents the data of Ref. 34 for the bulk critical field $H_c(T)$ scaled to $T_c = 1.177$ °K.

TABLE II. Parallel-critical-field temperature dependence.

Thickness (Å)	α	β (Oe)
1425	4.15	387
1750	3.16	370
2850	1.79	212
4000	1.42	160
6330	0.71	76
7000	0.69	83

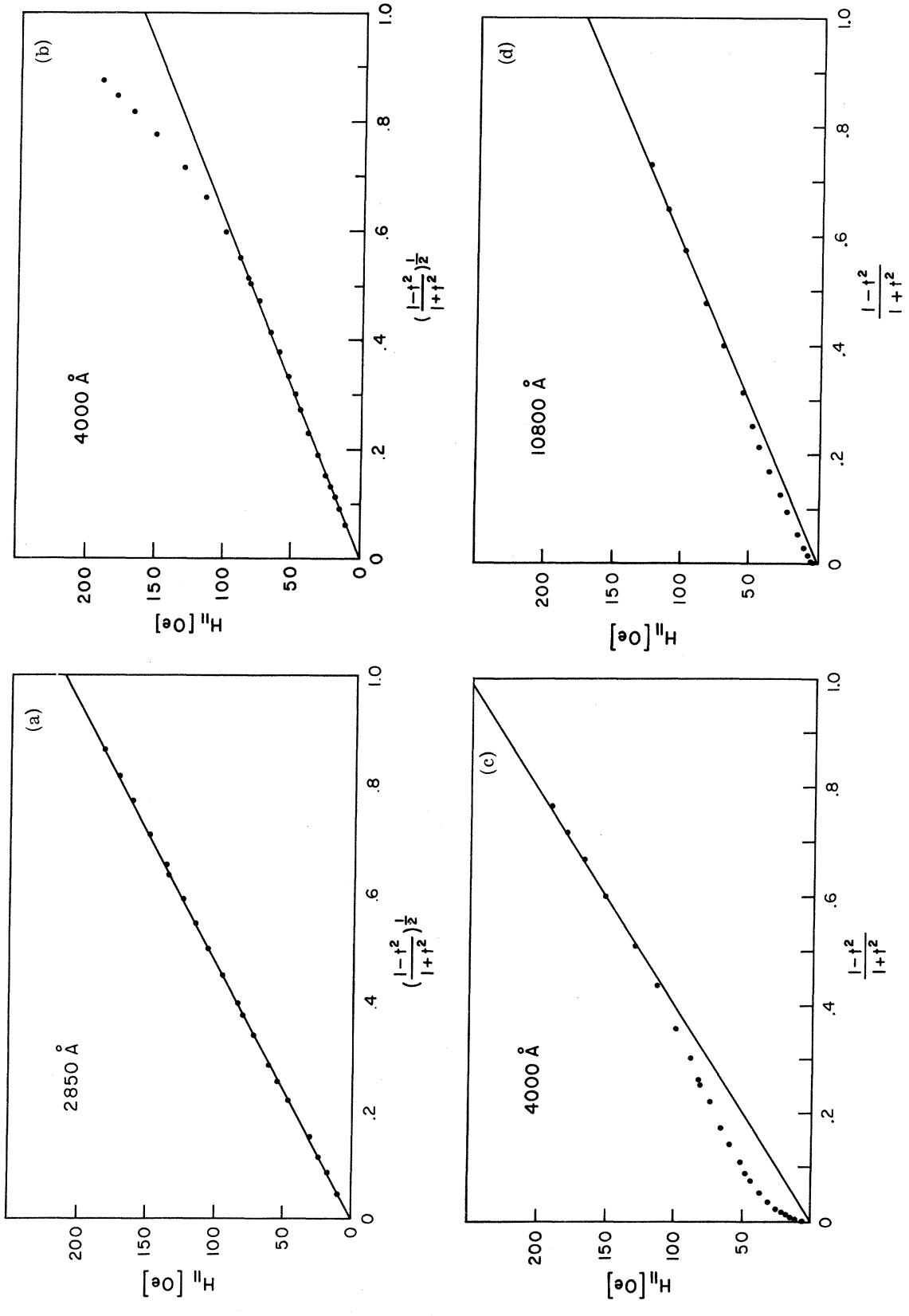

FIG. 4. Parallel critical fields of three films: (a) 2850-Å film plotted vs $[(1-t^2)/(1+t^2)]^{1/2}$. (b) 4000-Å film plotted vs $[(1-t^2)/(1+t^2)]^{1/2}$. Data depart from straight line below $t \simeq 0.73$. (c) 4000-Å film plotted vs $(1-t^2)/(1+t^2)$. Data become linear through the origin below $t \simeq 0.58$. (d) 10800-Å film plotted vs $(1-t^2)/(1+t^2)$.

$$H_{\parallel} = H_{c3} = 2.4\kappa H_c \ . \tag{12}$$

It is worthwhile to point out that this is a stronger temperature dependence than predicted by any microscopic theory.[36–38] Similarly stronger temperature dependences have been reported for a number of clean superconductors (Sn,[8] In,[8] Nb[39]) and attributed to Fermi-surface anisotropy.[40] It is unlikely that this explanation would hold in our case of "relatively dirty" films.

B. Perpendicular Orientation

1. *Films*

The film results (open circles) together with the foil results (solid circles) have been plotted in Fig. 5 in the form of $H_{\perp}/H_c$ as a function of thickness for five temperatures. We specify the distinction between film and foil behavior by emphasizing that the l of the foils exceeds that of the films by three orders of magnitude.

The perpendicular critical fields for films are seen to increase with decreasing thickness. We used Tinkham's expression[18] [Eq. (6)] to calculate the effective GL parameter $\kappa_{\perp}(t, l, d)$ for the seven films at eight different temperatures. The results are plotted vs $1/d$ in Fig. 6 for three of the eight temperatures. By extrapolating straight-line fits through the data to $d \to \infty$, we obtain $\kappa_{\perp}(t, l, \infty)$. These values have been plotted as a function of temperature in Fig. 7. At $t = 1$, $\kappa_{\perp}$ has been evaluated from

$$\kappa_{\perp}(1, l, d) = \lim_{t \to 1} \left(\frac{dH_{\perp}}{dt} \Big/ \sqrt{2}\, \frac{dH_c}{dt} \right) , \tag{13}$$

where $dH_{\perp}/dt$ was measured and dH_c/dT was taken from Harris and Mapother.[34]

2. *Foils*

The ratio $H_{\perp}/H_c$ for foils, represented by the solid circles in Fig. 5, falls considerably below unity as d decreases. The data at $t = 0.95$ and $t = 0.50$ have been plotted vs $1/\sqrt{d}$ in Fig. 8 in order to illustrate the linearity of this plot at $d \to \infty$ as required by Eq. (10). Values of the surface-energy parameter Δ at each temperature are denoted on the abscissa of Fig. 5 by triangles. The dashed curves drawn in Figs. 5 and 8 represent Eq. (8).

V. DISCUSSION

A. Films: Parallel Orientation

We use a nonlocal description[10] of the parallel critical field, valid for $d < d_c = \pi\lambda_{d_c}/\sqrt{2}$ and for $d < \xi(t, l)$ for the case of diffuse surface scattering, where $\lambda_{d_c} = \lambda_{eff}(t, l, d_c, \xi_0)$ is the effective penetration depth appearing in Eq. (3), evaluated at d_c. The function[10] f which is contained in λ_{eff} [see Eq. (4)], and which corrects for the nonlocal effects, is shown in Fig. 9. The case $d < d_c$ has been shown[10] to correspond to $H_{\parallel}/H_c > 2.2$. We also have $d < \xi(t, l)$ whenever $H_{\parallel}/H_c > 2.2$.

As mentioned in Sec. IV A 2, whenever $d < d_c(t)$ the parallel critical field obeys the two-fluid-model temperature dependence $H_{\parallel}(t) = \beta[(1 - t^2)/(1 + t^2)]^{1/2}$ within experimental error [see Figs. 4(a) and 4(b)]. Since the penetration depth decreases with temperature, only the thinnest samples satisfy $d < d_c$ at low temperatures. For thicker samples $H_{\parallel}$ becomes linear in $[(1 - t^2)/(1 + t^2)]^{1/2}$ only near $t = 1$. From the slopes β (Table II) and Eq. (5) we obtain the BCS coherence length ξ_0. The London penetration depth $\lambda_L(0)$ can then be obtained from the slopes α (Table II) and Eqs. (3) and (4). Similarly, one could have plotted $H_{\parallel}^2$ vs T near T_c and obtained $\lambda_{eff}(0)$ or $\lambda_L(0)$ for each sample from

$$H_{\parallel}^2 = 6\, \frac{\lambda_{eff}^2}{d^2} \left(\frac{dH_c}{dT} \right)^2 \Big|_{T_c} T_c(T - T_c) \ . \tag{14}$$

Alternatively, one could plot the data for all samples as $H_{\parallel}/H_c$ vs $f^{-1/2}(\xi_0/d)/d$ and obtain $\lambda_{eff}(t)$ for each temperature. All three possibilities agree within 10% with the quoted result (Sec. IV A 2). We observed that the thickness dependence of $H_{\parallel}$ was poorly represented by proportionality to either[11] d^{-1} or $d^{-3/2}$, but that $f^{-1/2}d^{-1}$ was satisfactory.

Having corrected for the effects of nonlocality and mfp, we can evaluate the GL parameter at $t = 1$, $l \to \infty$, and $d \to \infty$ from

$$\kappa_{\parallel} = 0.96\, \frac{\lambda_L(0)}{\xi_0} \ . \tag{15}$$

The average value for six films is $\kappa_{\parallel} = 0.086 \pm 0.02$. We have used $l = 0.15\ \mu$ for the above results. Due to the error in determining the mfp, we repeated the analysis for different values of l between 0.1 and 0.2 μ, and obtain different values of ξ_0 and $\lambda_L(0)$. The effect is only an additional 25% uncertainty in $\kappa_{\parallel}$.

For thicknesses and temperatures such that $d > 2\xi(t, l)$, the parallel critical field exhibits a different dependence on t and d. We have shown in Figs. 4(c) and 4(d) that $H_{\parallel}$ is proportional to $(1 - t^2)/(1 + t^2)$. Since the coherence length is larger than d near $t = 1$, no film data are linear near the origin. As the sample thickness decreases, $d > 2\xi$ obtains only at lower and lower temperatures. No samples less than 4000 Å thick are in this region for any temperature measured. In the range of large film thickness and low temperature we observe $H_{\parallel}/H_{\perp} = 1.7$, as expected from the theory of Saint-James and de Gennes.[14] Because of the small mfp, $\kappa(t, l, \infty)$ is large and we observe surface superconductivity with its critical field given by[14] Eq. (12). These results have been compared[35] to the "universal curve," which we discuss in Sec. V C.

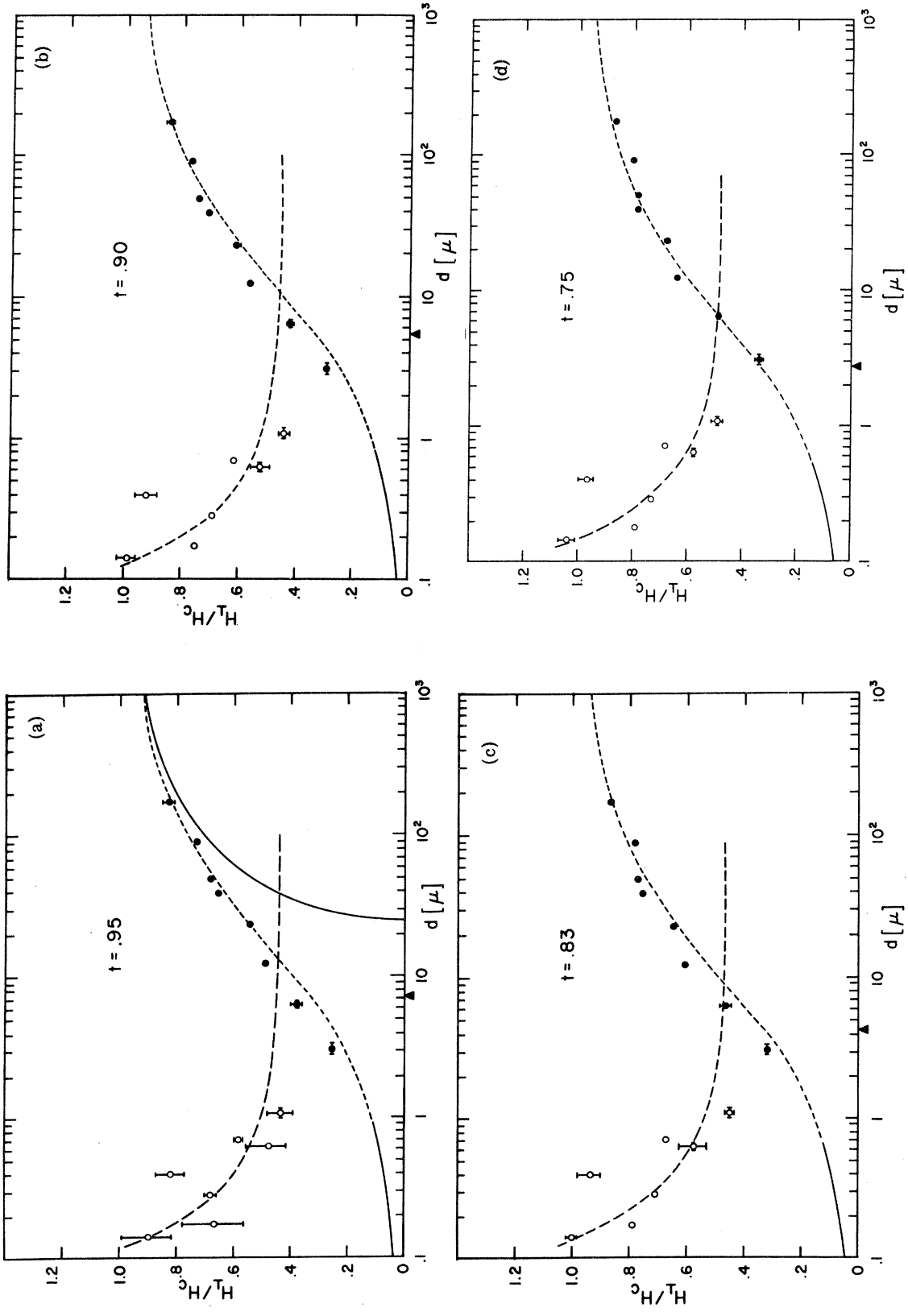

FIG. 5. Reduced perpendicular critical fields H_L/H_c as a function of sample thickness for five reduced temperatures. Solid circles and short-dashed curve represent foil data and theoretical fit. Open circles and long-dashed curve represent film data and theoretical fit. Solid curves are from theoretical asymptotic expressions. Triangles on the abscissa indicate the value of the surface-energy parameter at each temperature.

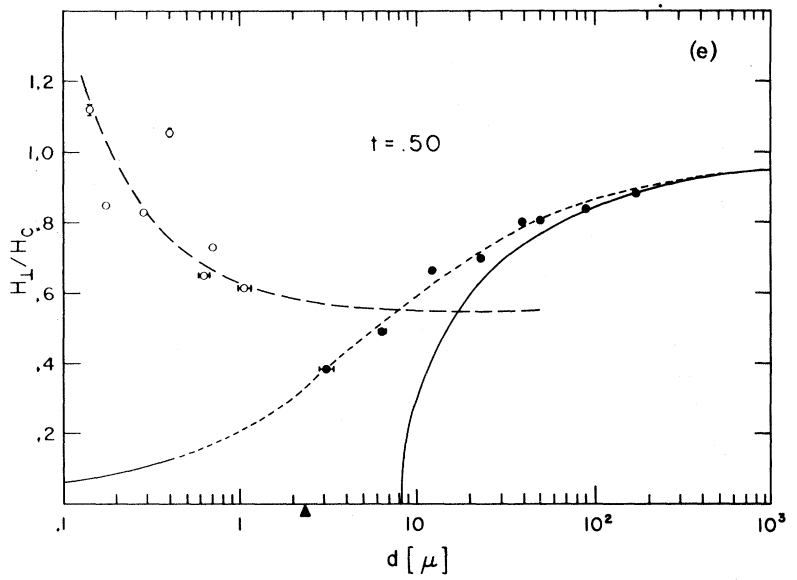

FIG. 5. (*Continued*)

B. Films: Perpendicular Orientation

The effective GL parameter $\kappa_\perp(t, l, d)$ was determined from our measurements of the perpendicular critical fields with Eq. (6). By assuming that boundary scattering and impurity scattering are equivalent, one can use Fuchs's[19] function to obtain an effective mfp for both processes. In our limit $l < d$, we get

$$\frac{1}{l_{\text{eff}}} = \frac{1}{l} + \frac{3}{8d}. \tag{16}$$

Koepke and Bergmann[41] have used this l_{eff} to obtain the approximation for $\xi_p < d$:

$$\kappa_\perp(t, l, d) = \kappa_\perp(t, l, \infty)\left(1 + \frac{3\xi_P}{8d}\right). \tag{17}$$

Extrapolations to $d \to \infty$ have been plotted in Fig. 7. At $t = 1$ we have $\kappa_\perp(1, l, \infty) = 0.30 \pm 10\%$. The uncertainty is the root-mean-square deviation for the straight-line fits in Fig. 6. Making Gor'kov's correction for the mfp we get $\kappa_\perp(1, l, \infty)\chi(\xi_0/l) = \kappa_\perp(1, \infty, \infty) = 0.086$, in striking agreement with the results for the parallel orientation. Again we have taken $l = 0.15$ μ. Other permitted values of l produce other values of $\kappa_\perp$, but for any particular value l' allowed by our estimated experimental error (i.e., $0.10\ \mu < l' < 0.20\ \mu$) we find $\kappa_\perp(l') = \kappa_{\text{II}}(l')$, to within 15%.

The dashed lines through the film data in Fig. 5 are the same as the straight-line fits in Fig. 6. According to Eq. (17) the slopes in Fig. 6 are given by $\frac{3}{8}\kappa_\perp(t, l, \infty)\xi_p$. We find disagreement with the parallel-field results for the coherence length, unless the numerical coefficient $\frac{3}{8}$ is increased by nearly a factor of 3. This discrepancy calls into question the fundamental assumption that the effective mfp for transport phenomena is the one to be used in Gor'kov's function χ. Gregory[42] has argued that Fuchs's[19] model improperly weights those electron paths in the plane of the sample. Hence the effective mfp should be smaller than that given by Fuchs. This suggests that a coefficient larger than $\frac{3}{8}$ is not unreasonable.

Dispersion in the results of films in perpendicular fields was attributed to variations in evaportion conditions, resulting in variations in the mfp from

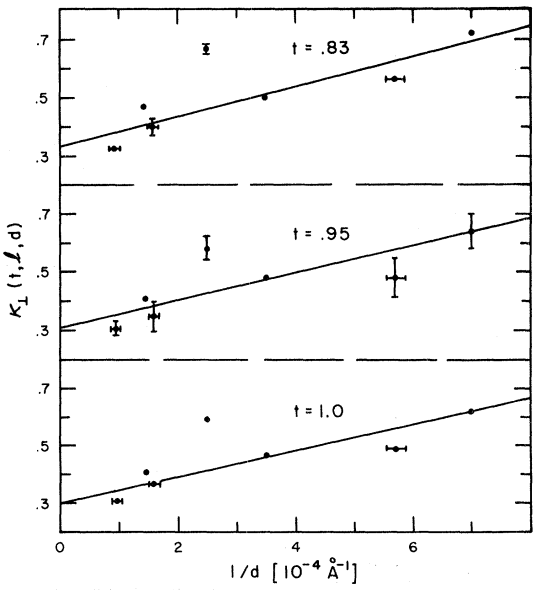

FIG. 6. Measured values of $\kappa(t, l, d)$ as a function of inverse film thickness $1/d$ at three reduced temperatures.

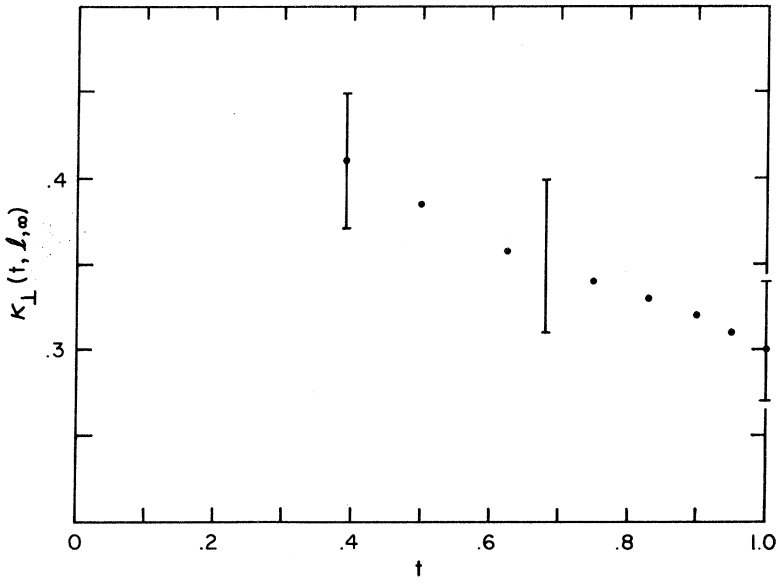

FIG. 7. Extrapolated values of $\kappa(t, l, \infty)$ as a function of reduced temperature t.

sample to sample. For example, the 4000-Å sample which deviates in Figs. 5 and 6 had an inordinately high resistivity. The dispersion in the parallel data was comparatively small.

C. Universal Curve

It can be seen in Fig. 7 that κ reaches 0.42 at low temperatures, where H_{c3} begins to exceed H_c [see Eq. (12)]. The thickest films approach this bulk limit and in parallel fields they seem to be in a surface-superconducting state. In this low-temperature–thick-film region $[d > 2\xi(t)]$ we measure the critical-field ratio $H_\parallel/H_\perp$ to be a constant equal to 1.7. This corresponds to the linear portion of the universal curve predicted by Saint-James and de Gennes.[14] A comparison of the results with the theory has been published elsewhere.[35]

One finds that the universal curve adequately describes the temperature and thickness dependence of the critical fields over the entire range of temperatures and film thicknesses measured. Near $t = 1$ the data approach the origin of the curve, whose x and y coordinates are proportional, respectively, to $H_\parallel(t)\, d^2$ and $H_\perp(t)\, d^2$. As the temperature decreases or the thickness increases, the data move away from the origin, finally reaching the linear

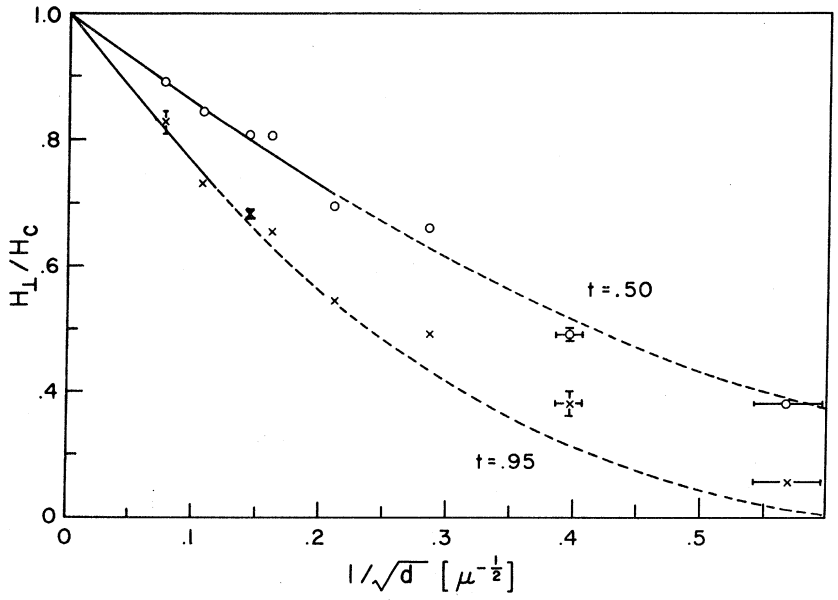

FIG. 8. $H_\perp/H_c$ vs inverse foil thickness $1/\sqrt{d}$ for two reduced temperatures: $t = 0.50$; $t = 0.95$. Dashed and solid curves represent theoretical fits.

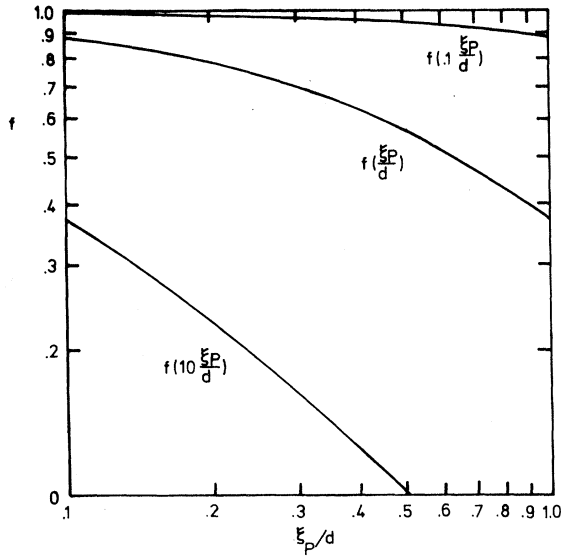

FIG. 9. Nonlocal correction factor for diffuse scattering calculated in Ref. 10 as a function of the ratio of the Pippard coherence length to sample thickness ξ_P/d. The curve has been split into three sections which correspond to three decades in the horizontal scale.

portion corresponding to a ratio of 1.7 at the lowest temperatures for the thickest samples.

We measured the critical field as a function of angle with respect to the plane of the sample, and we observed precise agreement with Tinkham's prediction[18] for a sample in the nonlinear portion of the universal curve.

D. Foils: Perpendicular Orientation

We have tried fitting Eqs. (9) and (10) to the measured perpendicular critical fields of our foils. In Fig. 8 we have plotted $H_\perp^D/H_c$ as a function of $d^{-1/2}$ for two different temperatures. Equation (10) gives a proper fit to the data over a rather limited range of thickness, thus supporting the theoretical restriction that Eq. (10) is valid only for $d \gg \Delta(t)$ and $\eta \to 1$. The asymptotic $d^{-1/2}$ dependence of the data extends to smaller thicknesses as the temperature [and therefore also $\Delta(t)$] decrease. Attempting to fit the data with Eq. (10) for all thicknesses can result in a large error in the determination of $C\Delta$.

Actually the result

$$\frac{H_\perp^D}{H_c} = \left\{1 + \frac{16\Delta}{\pi d}\left[1 + \left(1 + \frac{\pi d}{8\Delta}\right)^{1/2}\right]\right\}^{-2} \tag{18}$$

in disagreement with both Eqs. (9) and (10) has been calculated[12] in the limit $d \ll \Delta$. We have noticed, by solving Eq. (8) for thicknesses $d \ll \Delta$ with the values of ϕ calculated by Lifshitz and Sharvin,[21] that the ratios $H_\perp^D/H_c$ are in agreement with those predicted by Eq. (18). Therefore Eq. (8) gives the correct $H_\perp^D/H_c$ in both limits $d \gg \Delta$ and $d \ll \Delta$, and may be a good interpolation formula in the intermediate region. The validity of this conjecture is illustrated by Fig. 5, where we have plotted (short-dashed lines) the prediction of Eq. (8) with the ϕ of Ref. 21 over four decades of sample thickness. Equations (9) and (18) are also drawn as solid lines in Fig. 5, to emphasize the correct asymptotic behavior of Eq. (8) and also the difference between Eqs. (8) and (9). The agreement with the data is rather remarkable at all temperatures.

Let us analyze the possible implications of the agreement just presented. By extending Eq. (8) to small thicknesses we are assuming that the only thickness-dependent correction to the critical field is the surface-energy factor $(\Delta/d)^{1/2}$. The field-dependent factor, including the laminar shape, would remain thickness independent. That is, the magnetic energy contributions due to the distortion of the superconducting domains near the surface is assumed to be the same as that for an infinite sample in the presence of an applied field of magnitude $H_\perp^D$. Further progress in the theory of the intermediate state is required before the correctness of this interpretation can be known.

The surface-energy parameter Δ in Eq. (8) was obtained from the values of κ and λ from supercooling experiments[9] [$\lambda = 270/(1-t^4)^{1/2}$ Å] and the Ginzburg tabulation[24] of Δ/λ as a function of κ. No agreement between the foil data and Eq. (8) could be found when the values of κ and λ were taken from the film results.

Values for $C\Delta$ as a function of temperature were obtained from the limiting slopes in Fig. 8 together with Eq. (10). Calculating Δ from the values of κ and λ we get $C \simeq 3$, much larger than any theoretical model has given.[12]

We have applied our interpolation expression to Miller and Cody's data[3] for Sn. We find that if the supercooling values[8] for κ and λ are used one obtains good agreement between Eq. (8) (lower dashed line in Fig. 10) and their results for foils (solid points in Fig. 10). If the κ and λ are taken from their film analysis,[3] one finds good agreement between Eq. (8) (upper dashed line in Fig. 10) and their thick-film data (open points in Fig. 10).

Some interest has been devoted in the past,[2,3,6] to the critical thickness D_c, above which samples in perpendicular fields go into the intermediate state, and below which they are in the mixed state. By equating Eq. (8) for the intermediate-state solution to Tinkham's mixed-state solution[18] $\eta_c = \sqrt{2}\,\kappa_c$ at $d = D_c$, we obtain

$$\frac{D_c}{2\lambda} = \frac{\Delta}{\lambda}\,\frac{8\phi(\eta_c)}{(1-\eta_c)^4\,(1+\eta_c)^2}\,. \tag{19}$$

We have plotted D_c vs κ in Fig. 11 (upper curve),

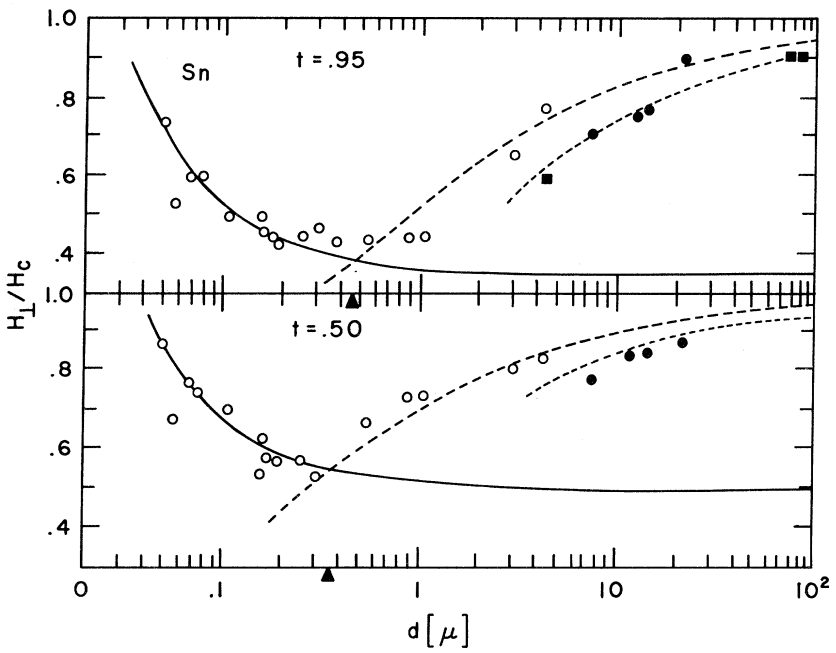

FIG. 10. $H_\perp/H_c$ data of Ref. 3 for Sn films, open circles and foils, closed circles, as a function of thickness. Dashed curves are from theory presented here. Solid curve is taken from Ref. 3. Triangles on abscissa mark the thickness D_c at which the curves intersect.

as obtained with Eq. (8) and using Ginzburg's[24] theory for Δ/λ vs κ.[43] For comparison the lower curve is drawn from Lasher's[13] calculation of the limiting case for which the mixed state can exist in increasing thicknesses. The curve labeled "Ginzburg" in Fig. 14 of Ref. 3 was obtained by using Eq. (10) for all thicknesses. We believe this incorrect ansatz for Δ leads to the spurious divergence of D_c for $\kappa \to 0$ shown in Ref. 3.

Included in the figure are values of D_c obtained for Sn (circles) and Pb (squares) by fitting Eq. (8) to the data of Cody and Miller,[2,3] as in Fig. 10. The triangles on the abscissa mark the intersection of the dashed and the solid lines. This procedure, instead of the use of Eq. (10) followed by Cody and Miller,[2,3] brings the results for Pb and Sn into basic agreement with our calculated curve. Because of the fundamental differences between our foil and film samples of Al, we cannot obtain experimental values of D_c, although by all indications estimates seem to fall on our calculated curve.

VI. SUMMARY AND CONCLUSIONS

The Al-film samples measured in this work exhibited second-order transitions in parallel and perpendicular fields. All showed strong size and mfp effects. From the measured $H_\parallel$ and H_c and a nonlocal theory we obtained λ_L, ξ_0, and $\kappa_\parallel$ for a pure infinitely thick film. From the measured $H_\perp$ and a semiempirical expression we obtained $\kappa_\perp$ for a pure thick film. $\kappa_\parallel$ and $\kappa_\perp$ were equal, but six times larger than the ideal bulk supercooling value κ_{sc}. A similar difference has been observed by others for Pb,[2] In,[6] and Sn.[3]

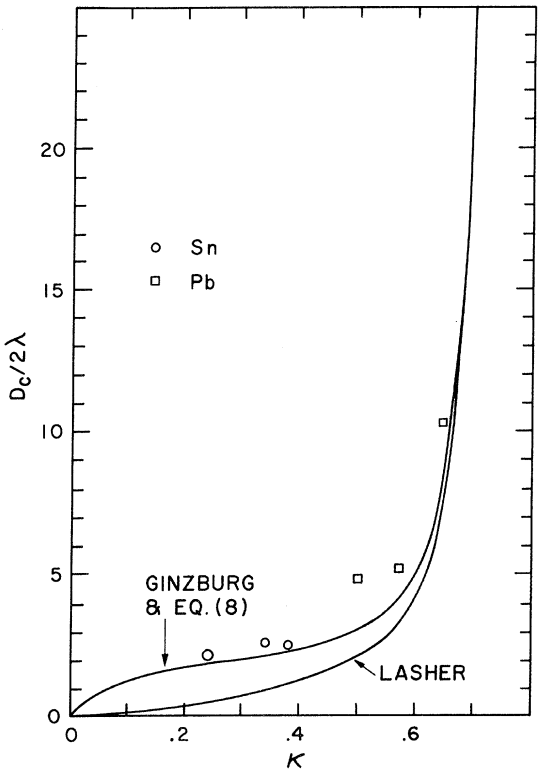

FIG. 11. Reduced critical thickness $D_c/2\lambda$ as a function of $\kappa(\infty)$. Lower curve is plotted from the theory given in Ref. 13. Upper curve is computed from Eq. (19) in the text using Ginzburg's calculation of the surface-energy parameter (Ref. 24). Data for Sn, open circles, and Pb, open squares, are obtained from curve fitting to the results of Refs. 2 and 3.

The foil samples exhibited first-order transitions in parallel and perpendicular fields. From the measured $H_\perp^D$ and a semiempirical expression we obtained Δ at several temperatures. This Δ is in agreement with that found with Ginzburg's[24] theory using for κ the pure bulk κ_{sc}.[9]

We have also considered the thickness D_c which corresponds to the change from first- to second-order transitions in perpendicular fields. Our semiempirical expression for $H_\perp/H_c$ leads to the result $D_c \to 0$ as $\kappa \to 0$, and restores general qualitative agreement between Ginzburg's[24] macroscopic and Lasher's[13] "microscopic" theory. It also brings the experimental estimates of D_c for Pb and Sn into better agreement with these theories.

The mfp of our films was small enough for the thick films to display surface superconductivity. We found the ratio $H_\parallel/H_\perp$ to be equal to 1.7, as expected. The behavior of all films at all temperatures was well described by the "universal curve" of Saint-James and de Gennes.[14] This affirms a consistency between our analyses of $H_\parallel$ and $H_\perp$. Since we believe the nonlocality is properly treated in obtaining $\kappa_\parallel$, then $\kappa_\parallel = \kappa_\perp$ indicates that the functional dependence $(1 + A/d)$ of the correction to $\kappa_\perp$ is probably acceptable. This means that the issue of localtiy will not explain the difference between $\kappa_\perp$ and κ_{sc}, in spite of the fact that the theoretical value of A may be questionable.

The discrepancy between κ_{sc} and $\kappa_\perp = \kappa_\parallel$ is not understood. An effect which may be related to this problem concerns the determination of ρl from size-dependent resistivity experiments. The measured ρl is always larger[27,44] than the value corresponding to bulk samples. This enhancement has been attributed[27,44] to mfp anisotropy. It is interesting to note from Eqs. (16) and (17) that ξ_p plays the role of l in correcting for the size effects on $\kappa_\perp$. The implication is that anisotropy may become important as ξ_p/d increases.[45]

There is some evidence to the contrary, however. In this experiment ξ_p has about the same value as that reported by Miller and Cody[3] for their Sn experiment. Yet the κ discrepancy for Al is a factor of 6 and for Sn the factor is only 2.5. In addition, the intermediate-state results seem to indicate that there is an intrinsic difference between evaporated and rolled or bulk samples. We were able to distinguish between the Sn film and foil data[3] and to identify the data with[3] $\kappa_\perp$ and[8] κ_{sc}, respectively. The purity was such that ξ_p was the same in both cases. It is difficult to explain the problem in terms of anisotropy effects alone.

Further experiments under controlled conditions of sample purity would be useful when coupled with measurements of the size-dependent resistivity.

ACKNOWLEDGMENTS

The authors acknowledge Professor A. Baratoff for helpful consultation and Professor G. M. Seidel for the use of his He^3 cryostat and magnet facilities. We are also indebted to G. D. Cody and R. E. Miller for copies of their preprints and data, and for a number of helpful discussions.

---

*Work supported by the Advanced Research Projects Agency and the U. S. Army Research Office, Durham, N.C.

†Now at the Institut für Experimentelle Kernphysik, 7500 Karlsruhe, West Germany.

‡Now at Centro Atomico Bariloche, San Carlos de Bariloche, Rio Negro, Argentina.

§Now at the Max Planck Institut für Festkörperforschung, 7000 Stuttgart 1, West Germany.

[1]V. L. Ginzburg, Zh. Eksperim. i Teor. Fiz. 34, 113 (1958) [Sov. Phys. JETP 7, 78 (1958)].

[2]G. D. Cody and R. E. Miller, Phys. Rev. 173, 481 (1968).

[3]R. E. Miller and G. D. Cody, Phys. Rev. 173, 494 (1968).

[4]G. K. Chang and B. Serin, Phys. Rev. 145, 274 (1965).

[5]J. P. Burger, G. Deutscher, E. Guyon, and A. Martinet, Phys. Rev. 137, A853 (1965).

[6]B. L. Brandt, R. D. Parks, and R. D. Chaudhari, J. Low Temp. Phys. 4, 41 (1971).

[7]J. Feder and D. S. McLachlan, Phys. Rev. 177, 763 (1969).

[8]F. W. Smith, A. Baratoff, and M. Cardona, Physik Kondensierten Materie 12, 145 (1970).

[9]F. de la Cruz, M. D. Maloney, and M. Cardona, in Conference on the Science of Superconductivity, Stanford University, 1969 (unpublished).

[10]R. S. Thompson and A. Baratoff, Phys. Rev. 167, 361 (1968); and unpublished.

[11]P. G. de Gennes and M. Tinkham, Physica 1, 107 (1964).

[12]E. Guyon, C. Caroli, and A. Martinet, J. Phys. (Paris) 25, 683 (1964).

[13]G. Lasher, Phys. Rev. 154, 345 (1967).

[14]D. Saint-James and P. G. de Gennes, Phys. Letters 7, 306 (1963).

[15]V. L. Ginzburg and L. D. Landau, Zh. Eksperim. i Teor. Fiz. 20, 1064 (1950).

[16]J. P. Burger and D. Saint-James, in *Superconductivity*, edited by R. D. Parks (Marcel Dekker, New York, 1969).

[17]L. P. Gor'kov, Zh. Eksperim. i Teor. Fiz. 37, 1407 (1959) [Sov. Phys. JETP 10, 998 (1960)].

[18]M. Tinkham, Phys. Rev. 129, 2413 (1963); Rev. Mod. Phys. 36, 268 (1964).

[19]K. Fuchs, Proc. Cambridge Phil. Soc. 34, 100 (1938).

[20]P. G. de Gennes, *Superconductivity of Metals and Alloys*, translated by P. A. Pincus (Benjamin, New York, 1966).

[21]E. M. Lifshitz and Yu. V. Sharvin, Dokl. Akad. Nauk SSSR 79, 783 (1951).

[22]L. D. Landau, Zh. Eksperim. i Teor. Fiz. 7, 371 (1937).

[23]E. A. Davies, Proc. Roy. Soc. (London) A255, 407 (1960).

[24]V. L. Ginzburg, Physica 24, S42 (1958).
[25]J. Bardeen, Phys. Rev. 94, 554 (1954).
[26]A. V. Bassewitz and G. V. Minnigerode, Z. Physik 181, 368 (1964).
[27]P. Cotti, E. M. Fryer, and J. L. Olsen, Helv. Phys. Acta 37, 585 (1964).
[28]I. Holwech and J. Jeppesen, Phil. Mag. 15, 217 (1967).
[29]R. Reich and F. Montariol, Compt. Rend. 254, 3357 (1962).
[30]A. Von Bassewitz and E. N. Mitchell, Phys. Rev. 182, 712 (1969).
[31]D. Markowtiz and L. P. Kadanoff, Phys. Rev. 131, 563 (1963).
[32]I. S. Khukhareva, Zh. Eksperim. i Teor. Fiz. 43, 1173 (1962) [Sov. Phys. JETP 16, 828 (1963)].
[33]M. Strongin, O. F. Kammerer, and A. Paskin, Phys. Rev. Letters 14, 949 (1965).
[34]E. P. Harris and D. E. Mapother, Phys. Rev. 165, 522 (1968).
[35]M. D. Maloney and F. de la Cruz, Solid State Commun. 9, 1647 (1971).
[36]L. P. Gorkov, Zh. Eksperim. i Teor. Fiz. 37, 883 (1959) [Sov. Phys. JETP 10, 593 (1960)].
[37]E. Helfand and N. R. Werthamer, Phys. Rev. 147, 288 (1966); Phys. Rev. Letters 13, 686 (1964).
[38]G. Eilenberger, Phys. Rev. 153, 584 (1967); Z. Physik 190, 142 (1966).
[39]G. W. Webb, Solid State Commun. 6, 33 (1968).
[40]P. C. Hohenberg and N. R. Werthamer, Phys. Rev. 153, 493 (1967).
[41]R. Koepke and G. Bergmann, Z. Physik 242, 31 (1971).
[42]W. D. Gregory, Phys. Rev. Letters 20, 53 (1968); W. D. Gregory, M. A. Superata, and P. J. Carroll, Phys. Rev. B 1, 85 (1971).
[43]To use the Ginzburg theory it is assumed that $\kappa(d_c) \simeq \kappa(\infty)$.
[44]R. T. Bate, B. Martin, and P. F. Mille, Phys. Rev. 131, 1482 (1963).
[45]The authors thank A. Baratoff for this suggestion.

PHYSICAL REVIEW B VOLUME 5, NUMBER 9 1 MAY 1972

Stability of Supercurrents in Cylindrical Films of Tin†*

H. Lawrence Phillips‡ and Hans Meissner
Department of Physics and Cryogenics Center, Stevens Institute of Technology, Hoboken, New Jersey 07030
(Received 7 September 1971)

Using current pulses with a rise time of less than 0.5 nsec and a pulse length of 240 nsec, the stability of supercurrents in cylindrical films of tin has been investigated. For current densities J in excess of the instability current density $J_I = J_I(0)\,[1-(T/T_c)^4]$, the sample voltage rises with time as $a(J,T)f(t/t')$, where $f(t/t')$ is a universal function of t/t'. The time constants t' cover a range of 0.5 nsec $< t' <$ 200 nsec. The amplitude coefficients a rise from zero as J exceeds J_I and then join onto the values $a = iR_n$, the voltage in the normal state. The time constants t' depend on current and temperature as $t' \approx t_0[J_I'/(J-J_I) - \epsilon J_I^2/(J-J_I)^2]$, where $J_I(0)$ has values of the order of 15×10^5 A/cm^2 and $t_0 \approx 14$ nsec, while $\epsilon \sim 3\times10^{-3}$.

I. INTRODUCTION

It has been found that for superconducting films there are three current densities of interest[1-4]: (i) a current density J_p at which flux tubes break free from their pinning sites with resulting flux flow and flux-flow resistivity; (ii) a current density J_I at which an instability occurs. The most prominent feature of this instability is the increase of the voltage along the film with time, even though the current is kept constant[1,3]; (iii) a current density J_c which is the theoretical critical current density as calculated from Ginzberg-Landau theory.[5] The present work deals with the instability current. Cylindrical samples were used since for flat samples there are two different types of instabilities, one which seems to be quite general and one arising from the edges of the film.[3] For cylindrical samples it is known[2] that there is only one instability down to 1.2 K. Also, with cylindrical samples it is possible to keep accidental perpendicular components of the magnetic field extremely low and therefore not to be disturbed by flux flow.

The first study of this instability[2] was restricted by the use of current pulses which had a ratio of pulse length to rise time of only 13. This prevented observation of the time constants over a sufficiently large range and had an uncontrolled influence on the early part of the voltage rise. In the present experiment the current pulse rises in less than 0.5 nsec and stays substantially constant for the rest of the pulse, 240 nsec. With this improvement it is now possible to show that all voltage V vs time t curves have the same shape: $V(t) = af(t/t')$, where the time constants t' cover a range of 0.5 nsec $< t' <$ 200 nsec, depending on current and temperature. The function $f(t/t')$ is similar to, but distinctly different from, the error